BIOCHEMISTRY
including biophysical chemistry & molecular biology

Article

pubs.acs.org/biochemistry

Structural Studies of Hydroxylamine Oxidoreductase Reveal a Unique Heme Cofactor and a Previously Unidentified Interaction Partner

Peder Cedervall,[†] Alan B. Hooper, and Carrie M. Wilmot*

Department of Biochemistry, Molecular Biology, and Biophysics, University of Minnesota, Minneapolis, Minnesota 55455, United States

Supporting Information

ABSTRACT: Hydroxylamine oxidoreductase (HAO) is a 24-heme homotrimeric enzyme that catalyzes the conversion of hydroxylamine to nitrite in nitrifying bacteria: a key reaction in the nitrogen cycle. One heme in each HAO monomer is a highly unusual heme P460 that is the site of catalysis. This was proposed to be a *c*-type heme that contained an additional porphyrin−tyrosine cross-link. Here, we report the crystal structure of HAO from *Nitrosomonas europaea* to 2.1 Å resolution that defines a different model compatible with the crystallographic and biochemical data. The structure reveals that heme P460 contains two covalent cross-links between the porphyrin and a Tyr residue. In addition, the enzyme was purified from source, and an unknown physiological HAO binding partner was present within the crystal (annotated in the genome as hypothetical protein NE1300). NE1300 may play a structural role in the ternary complex with cytochrome c_{554}, the physiological electron acceptor of HAO.

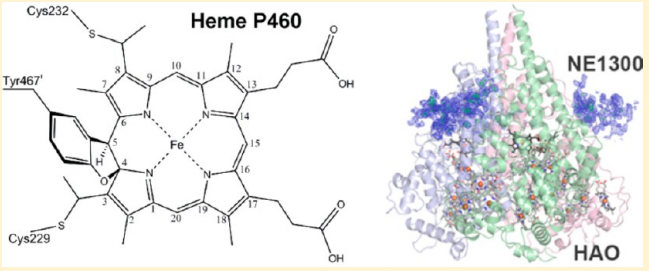

Ammonia oxidation is rate-limiting in nitrification in many diverse environments, making it an important component of global inorganic nitrogen cycling.[1] In nitrifying bacteria, ammonia is first oxidized to hydroxylamine by ammonia monooxygenase (AMO) located in the cytoplasmic membrane (Figure 1). Hydroxylamine is subsequently oxidized to nitrite by hydroxylamine oxidoreductase (HAO). Each turnover of HAO yields four electrons, which are transferred to the tetraheme electron transport protein cytochrome c_{554} (Cyt c_{554}).[2,3] Both HAO and Cyt c_{554} are soluble enzymes found in the periplasmic space of the bacterium. Two of HAO's product electrons are subsequently transferred back to AMO as substrate electrons, and the other two electrons contribute to the electrochemical gradient through a terminal oxidase in the cytoplasmic membrane. It is noteworthy that HAO is the only known enzyme that can withdraw electrons from a heme-ligated substrate during turnover.[4]

A crystal structure of HAO from *Nitrosomonas europaea* to 2.8 Å resolution showed a homotrimeric protein with eight hemes (I−VIII) per 67 kDa monomer (Supporting Information Figure S1).[5] Seven of the eight hemes per subunit (I−III and V−VIII) are *bis*-His coordinated *c*-type hemes and are likely involved in transferring the product electrons from the catalytic heme IV to Cyt c_{554}.[5,6] The charge and geometry of the HAO surface around the solvent exposed heme I is complementary to that of Cyt c_{554}.[7] This suggests that each HAO molecule forms a complex with three Cyt c_{554} molecules and that the electrons are transferred to the cytochrome through heme I.

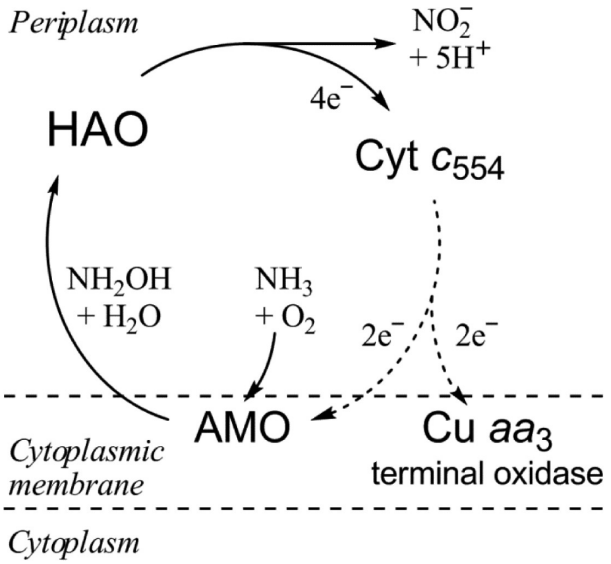

Figure 1. Ammonia oxidation in nitrifying bacteria. Cu aa_3: aa_3-type cytochrome *c* oxidase.

The catalytic heme IV in HAO is named heme P460 due to the λ_{max} of its ferrous Soret band.[8,9] On the basis of mass

Received: July 18, 2013
Revised: August 13, 2013
Published: August 18, 2013

   dx.doi.org/10.1021/bi400960w | *Biochemistry* 2013, 52, 6211−6218

spectrometry (MS), N-terminal sequencing, and nuclear magnetic resonance spectroscopy (NMR) of proteolyzed HAO fragments, it was proposed that heme P460 is a *c*-type heme with an additional covalent bond to the protein.[10] The MS data showed that the additional modification results in a net loss of two protons. NMR data suggested that one of the two protons originated from a tyrosyl aromatic ring carbon, and the other proton from a *meso* carbon of the porphyrin. In the subsequent 2.8 Å crystal structure, the cross-link was modeled between Tyr-C3 and porphyrin-C5 (Figure 2).[5] The Tyr

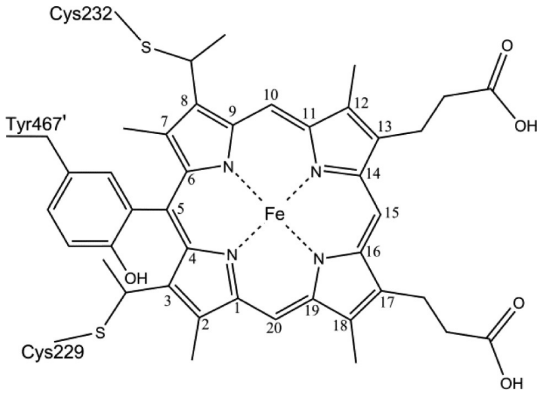

Figure 2. Chemical drawing of HAO heme P460 based on MS, NMR spectroscopy, and the previously determined 2.8 Å resolution X-ray crystal structure.[5,10].

residue is from the adjacent subunit (Tyr467′, where ′ denotes that the residue is from an adjacent subunit), thereby covalently cross-linking the three protomers together.

Another protein found in *N. europaea* and other bacteria, cytochrome P460 (Cyt P460), illustrates the apparent relevance of the heme−peptide cross-link to an oxidative function. Cyt P460 is unrelated to HAO and contains a single *c*-type heme with a ferrous optical absorption band at 460 nm.[11,12] The physiological function of Cyt P460 has not been established, but it has the ability to catalyze hydroxylamine oxidation.[13,14] In *N. europaea*, the heme of Cyt P460 has a third cross-link to the protein between the amine nitrogen of a Lys residue and porphyrin-C15 (opposite meso carbon to heme P460 of HAO, Figure 2).[12,15] A severe steric clash in the published 2.8 Å resolution HAO structural model between the hydroxyl group of Tyr467′ and the porphyrin and the different properties of an aromatic ring carbon of Tyr467′ (in HAO) compared with those of a primary amine nitrogen of Lys70 (in *N. europaea* Cyt P460) prompted us to reassess the current HAO heme P460 model using a new HAO crystal form that diffracts to higher resolution.

EXPERIMENTAL PROCEDURES

Expression, Purification, and Crystallization. The expression and purification of HAO from *N. europaea* was carried out as previously described.[16] Briefly, *N. europaea* cells were disrupted by freeze−thawing (from −10 to 4 °C). The resulting cell homogenate was centrifuged at 20000*g* for 20 min and the supernatant was fractionated with ammonium sulfate. The 60−80% saturated ammonium sulfate precipitate was resuspended in 50 mM potassium phosphate buffer, pH 7.5, and then dialyzed against 10 mM potassium phosphate buffer, pH 7.5. This was then subjected to a Sephadex G-100 column equilibrated with 200 mM potassium chloride and 50 mM potassium phosphate buffer, pH 7.5. The fractions containing HAO were concentrated by ultracentrifugation and loaded onto a Sepharose CL-6B column equilibrated with 200 mM potassium chloride and 50 mM potassium phosphate buffer, pH 7.5. The second gel-filtration chromatography step was followed by ion exchange chromatography on a DEAE-Sephacel column equilibrated with 20 mM Tris−Cl, pH 8.1. Homogeneous HAO was eluted with a 0−300 mM sodium chloride gradient. The protein was stored in −80 °C for 13 years before being thawed and used for crystallization. The protein was handled and crystallized as described in Cedervall et al.[17] In short, a single plate-shaped crystal was grown in a 72-well microbatch plate containing 2 μL protein and 2 μL crystallization solution (0.1 M potassium nitrate, 0.1 M MES−Na buffer, pH 7.5, and 46% (v/v) PEG 400). The crystal was flash cooled in liquid N_2 without any additional cryoprotectant.

X-ray Diffraction Data Collection and Processing. X-ray diffraction data were collected at the Structural Biology Center beamline 19-ID-D at the Advanced Photon Source, Argonne National Laboratory, Argonne, IL. A total of 120° of data were collected from a single crystal using an ADSC-CCD detector. Data collection was done with a 100 × 100 μm beam at cryogenic temperatures (100 K). The data were processed as orthorhombic $P2_12_12$ with unit cell parameters a = 140.7, b = 142.6, and c = 107.4 Å using HKL2000.[18] X-ray data collection and processing statistics are shown in Table 1.

Data Analysis, Model Building, and Refinement. Analysis of the scaled diffraction data was carried out using programs in the Collaborative Computational Project Number 4 (CCP4) suite.[19] Cell content analysis (Matthews) suggested that the asymmetric unit contained three HAO monomers. Initial phases were generated with Phaser using one monomer from the previously determined crystal structure (PDB ID: 1FGJ) as the search model, but with all nonpolypeptide molecules removed.[5] The automated search in Phaser gave the strongest solution for space group $P2_12_12$, placing three monomers in the asymmetric unit (ASU). Rigid body refinement using the homotrimeric model located by Phaser gave initial R-values of 29% for both R_{work} and R_{free}. All the expected heme binding sites showed strong positive $F_o - F_c$ electron density, signifying the correctness of the solution. To minimize model bias, Tyr467′ (where ′ denotes that the residue is from an adjacent subunit) involved in the protein−heme P460 cross-link was truncated to Ala. In the early stages of refinement, the seven regular *c*-type hemes per subunit were included in the model with the thioether links restrained to 1.84 Å. Once refinement of the HAO model was almost complete, regular *c*-type hemes were placed in the electron density at the expected heme P460 sites and residue 467′ converted back to Tyr. The electron density agreed with the two-cross-link model, including sp^3 hybridization at C4 and C5 of the porphyrin. Heme P460 library files for use in refinement were created using Library Monomer Sketcher in the CCP4 suite. Tyr467′-C3−porphyrin-C5 and Tyr467′-O−porphyrin-C4 links were restrained to 1.47 and 1.50 Å, respectively. The protein−heme P460 thioether links were restrained to 1.84 Å as expected for regular *c*-type hemes. The two-cross-link Tyr467′ is at 100% occupancy, as judged by *B*-factors being comparable to those of the heme and the absence of negative $F_o - F_c$ electron density. HAO is predicted to contain 546 residues, and residues 1−502 could be built into the electron density. The crystal packing had limited space for the missing C-terminal residues, so the possibility that the HAO sample used for

Table 1. X-ray Crystallography Data Collection and Refinement Statistics[a]

Data Collection	
space group	$P2_12_12$
unit cell lengths (Å)	140.7 × 142.6 × 107.4
unit cell angles (deg)	90.0
wavelength (Å)	0.979 48
resolution (Å)	50.00−2.10 (2.14−2.10)
unique reflections	109 103
completeness (%)	86.7 (69.3)
multiplicity	4.6 (3.9)
R_{merge} (%)[b]	12.7 (57.4)
$I/\sigma I$	9.6 (2.0)
Refinement	
resolution (Å)	42.89−2.10 (2.16−2.10)
no. reflections; working/test	95 555/5 071
R_{work} (%)[c]	16.5
R_{free} (%)[d]	20.6
protein atoms	13 133
ligand atoms	1279
solvent sites	785
Ramachandran statistics[e]	
favored/allowed (%)	95.91/3.48
outliers (%)	0.61
rmsd	
bond lengths (Å)	0.023
bond angles (deg)	2.102
average B-factor (Å^2)	37.3
estimated standard uncertainty (Å); R_{work}/R_{free}	0.251/0.189
PDB ID	4FAS

[a]Values in parentheses are for the highest resolution shell. [b]$R_{merge} = \sum_i|I_{hkl,i} - \langle I_{hkl}\rangle|/\sum_{hkl}\sum_i I_{hkl,i}$, where I is the observed intensity and $\langle I_{hkl}\rangle$ is the average intensity of multiple measurements. [c]$R_{work} = \sum||F_o| - |F_c||/\sum|F_o|$, where $|F_o|$ is the observed structure factor amplitude and $|F_c|$ is the calculated structure factor amplitude. [d]R_{free} is the R-value based on 5% of the data excluded from refinement. [e]Based on values attained from refinement validation options in COOT.

crystallization was not full length was considered. Proteolysis/MS analysis of the HAO SDS-PAGE gel band detected no peptides containing residues beyond residue Ser507 (Supporting Information Figure S2). Because the sample was treated with trypsin (primarily cleaves C-terminal of Lys and Arg), this is suggestive evidence for Ser507 being the C-terminus of the HAO sample, consistent with the crystal packing.

A 42-residue poly-Ala chain was initially modeled into each of the three unexplained protein electron density regions that were not part of the HAO trimer. Following NE1300 identification, the electron density was consistent with the amino acid sequence, and the poly-Ala model was replaced. The electron density was somewhat weak for parts of NE1300, and so noncrystallographic symmetry (NCS) averaged electron density maps were used in the modeling process. Model building and generation of NCS maps were done in Crystallographic Object-Oriented Toolkit (COOT).[20] For refinement, REFMAC[21] in the CCP4 suite was used. A random sample of 5% of the data across all resolution shells was chosen as an unbiased check to track refinement through calculation of an R_{free}. The remaining 95% of the reflections were used in refinement (R_{work}). At the later stages of refinement, translation−libration−screw (TLS) refinement was introduced.[22] Model refinement statistics are shown in Table 1. The atomic coordinates and the structure factors have been deposited in the Protein Data Bank as entry 4FAS.

Model Analysis. Structural alignments were done in PyMOL.[23] The displacements along the lowest-frequency normal coordinates of the porphyrin macrocycle of heme P460 were analyzed using the online normal-coordinate structure decomposition (NSD) engine, version 3.0, at http://jasheln.unm.edu/jasheln/content/nsd/NSDengine/start.htm.[24,25] Heme P460 was, as recommended for all protoporphyrin IX (*b*-type heme) related molecules, oriented so the ethyl groups are in quadrants I and II in the structure window in the NSD program. The surface area of NE1300 partitioning in the NE1300−HAO interface (area of NE1300 within 4 Å of HAO) was calculated using PyMOL. The type of intermolecular interactions present at the interface was established using the protein interactions calculator server at http://pic.mbu.iisc.ernet.in/job.html.[26] The protein−protein interface between HAO and NE1300 is mainly hydrophobic in nature, with an interaction surface of about 1000 Å^2, close to 25% of the total surface area of NE1300 visible in the electron density.

Molecular Docking. For the HAO−NE1300−Cyt c_{554} complex, illustrations in Iverson et al.[7] were used as a guide to roughly position Cyt c_{554} in one of the three proposed docking sites on the experimental HAO−NE1300 hexameric model. The resulting pdb-file was uploaded to the Rosetta protein−protein docking server (http://rosettadock.graylab.jhu.edu/).[27] The docking server output pdb-file was used to generate a symmetric nonameric HAO−NE1300−Cyt c_{554} complex.

N-Terminal Sequencing and Mass Spectrometry. N-terminal sequencing was done at the Oligonucleotide and Peptide Synthesis Facility, BioMedical Genomics Center at the University of Minnesota. The sample was separated in a 12% Bis−Tris SDS-PAGE gel and blotted onto a Sequi-Blot PVDF membrane. The membrane was stained using a solution of 0.1% Amido Black 10B solution. The band on the PVDF membrane thought to correspond to the identified binding partner to HAO was cut out and analyzed through 10 cycles of Edman degradation followed by reversed-phase HPLC. In-gel proteolysis (trypsin) followed by MS analysis was carried out at Taplin Biological Mass Spectrometry Facility at Harvard Medical School, Boston, MA. The bands sent for in-gel proteolysis/MS were generated in a 4−12% Bis−Tris SDS-PAGE gel for the HAO trimer and a 12% Bis−Tris SDS-PAGE gel for the HAO binding partner. The gels were stained with SimplyBlue SafeStain.

Primary Sequence Analysis. Transmembrane helix prediction in HAO was done using TopPred at http://mobyle.pasteur.fr/cgi-bin/portal.py?form=toppred. To identify the protein binding partner to HAO, the results from the N-terminal sequencing and mass spectrometry were analyzed using blastp (protein−protein BLAST) at http://blast.ncbi.nlm.nih.gov/Blast.cgi.

RESULTS

Overall Structure of Hydroxylamine Oxidoreductase. The model was refined against the diffraction data out to 2.1 Å resolution with R_{work} and R_{free} of 16.5% and 20.6%, respectively. The statistics for X-ray diffraction data collection, processing, and refinement are presented in Table 1. The HAO model is very similar to the previously published 2.8 Å resolution model with an rmsd between monomers of 0.41 Å (Figure 3).[5] The

dx.doi.org/10.1021/bi400960w | *Biochemistry* 2013, 52, 6211−6218

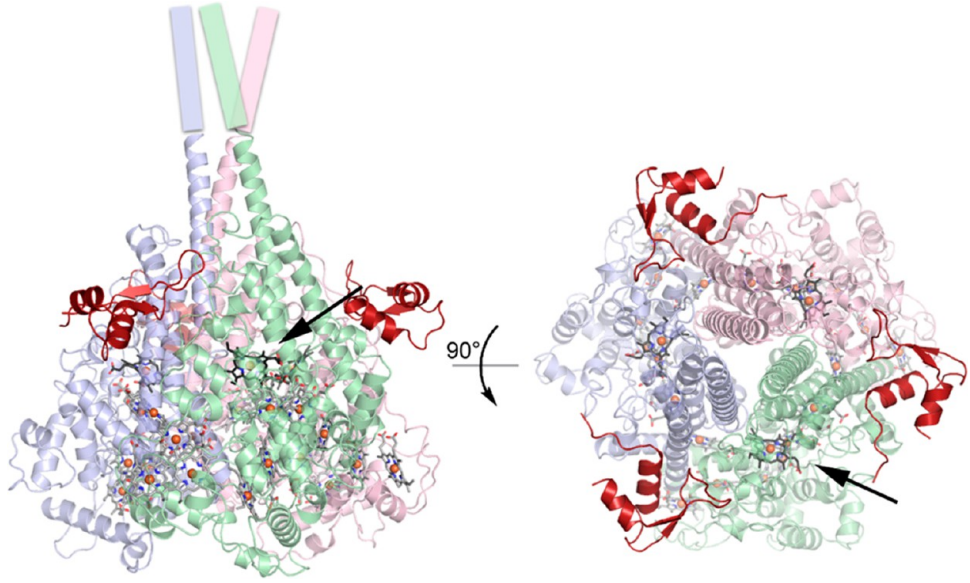

Figure 3. Overall HAO structure with NE1300. The protein is drawn as a cartoon. The HAO trimer is faded and colored by subunit (pink, green,and blue), and the NE1300 is in red. The hemes are drawn as sticks colored by atom (carbon: *c*-type hemes (I–III and V–VIII), light gray; catalytic heme P460 (IV), dark gray). The Fe of the hemes are drawn as orange spheres. The arrows indicate the position of the active site pocket in one of the three subunits. The pink, green, and blue cylinders illustrate residues 508–546 of the C-terminus of HAO that were not present in the protein used for crystallization. This figure was generated in PyMOL, http://www.pymol.org.[23]

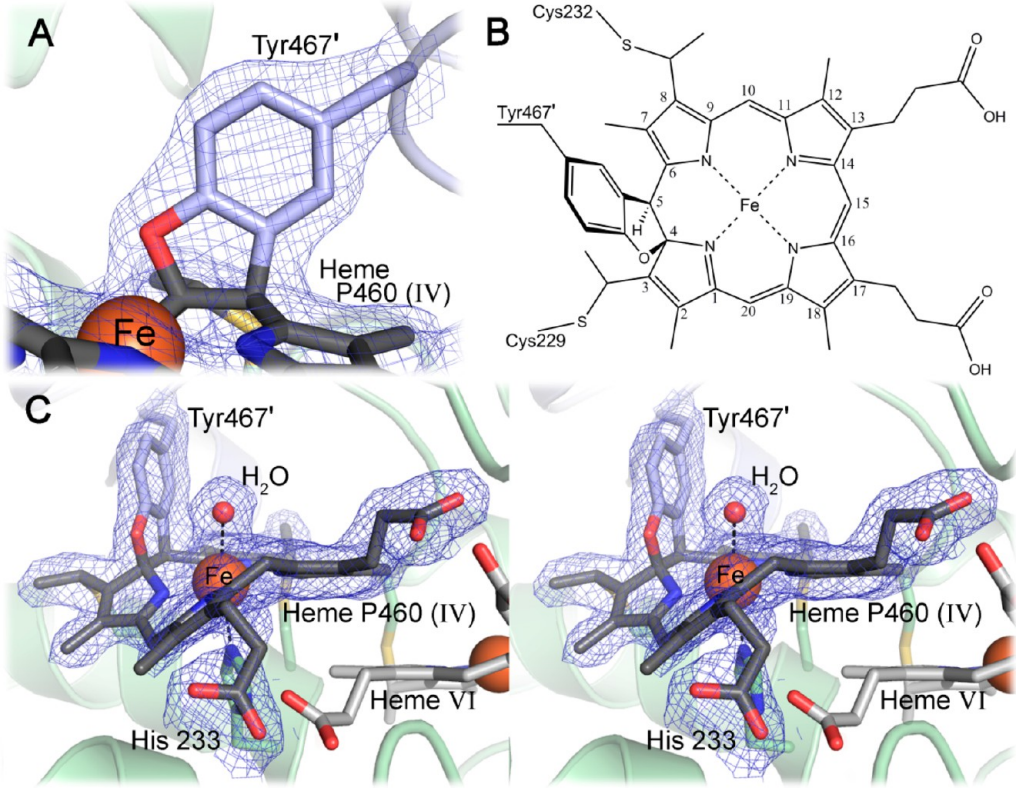

Figure 4. HAO heme P460 double cross-link model. (A) Close-up view of the heme P460–Tyr double cross-link. (B) Chemical drawing of heme P460. (C) Stereoview of heme P460 seen from the opening of the active site pocket. The protein is drawn as faded cartoon colored by subunit (green and blue). The hemes and amino acids are drawn as sticks colored by atom (carbon: amino acid side chains, as subunit (green and blue); heme VI, light gray; heme P460 (IV), dark gray). The Fe of the hemes are drawn as orange spheres. The Fe-coordinating water molecule is represented by a red sphere. The $2F_o - F_c$ electron density contoured at $+1\sigma$ is drawn as blue mesh. Panels A and C were generated in PyMOL, http://www.pymol.org.[23]

2.8 Å resolution model contains 499 residues (residue 1–499 out of the 546 encoded by the *hao* open reading frame). This is comparable to the model presented here in which the first 502 residues could be modeled into the electron density map. To

dx.doi.org/10.1021/bi400960w | *Biochemistry* 2013, 52, 6211–6218

check for truncation, the HAO sample was subject to proteolysis/MS analysis, which indicated that the C-terminus was at Ser507 (Supporting Information Figure S2). Although the vast majority of HAO is present in a soluble form in vivo, it has been reported that under certain growth conditions (low Fe/low Cu), some HAO appears to be associated with the cytoplasmic membrane.[28] Interestingly, a transmembrane helix is predicted in the C-terminal part that is missing in the sample used in this study (Supporting Information Figure S3).[29] Therefore, HAO may be post-translationally cleaved after Ser507 in vivo to yield the soluble form of the enzyme, as suggested by the MS result. Limiting metals during growth could restrict the maturation of HAO, with the membrane-bound form representing incompletely processed enzyme.[28]

Structure of Heme P460. The electron density confirmed the presence of the Tyr467′-C3−porphyrin-C5 cross-link but indicated an additional cross-link between the hydroxyl Tyr467′-O and C4 of the porphyrin (Figure 4). The Tyr467′-C3−porphyrin-C5 and Tyr467′-O−porphyrin-C4 distances refined to an average of 1.5 Å across the three active sites in the ASU. The aromaticity of the porphyrin is clearly disrupted, with both C4 and C5 of the porphyrin being sp^3 hybridized. Single crystal spectra taken before and after X-ray data collection clearly demonstrated that the 21 *c*-type hemes were undergoing photoreduction in the beam (Supporting Information Figure S4). Deconvolution of the λ_{max} of the three hemes P460 from the Soret absorption band of the normal *c*-type hemes in the crystals was ambiguous. Therefore, although likely, it is uncertain whether heme P460 was also in the ferrous state.

The electron density also indicates that the distal side of heme P460 is occupied by a water molecule (Figure 4C). In the previously reported HAO crystal structure, the Fe atom of heme P460 was described as pentacoordinated, but at 2.8 Å resolution the authors were unable to model ordered water.[5] The hexacoordinated HAO heme P460 reported here is consistent with the DFT study that supported an aquo ferric state,[30] although the structure may reflect the ferrous state of heme P460 due to photoinduced reduction in the X-ray beam (Supporting Information Figure S4).

Structure of NE1300. Electron density that could not be explained by the HAO molecule was detected next to the HAO trimer (Supporting Information Figure S5). The authors of the previously reported HAO structure also detected electron density that they speculated could be the missing 47 residues of the C-terminus.[5] SDS-PAGE of the protein sample and dissolved crystals revealed the presence of a small polypeptide with a molecular weight of about 7 kDa (Supporting Information Figure S6) that was excised and subjected to N-terminal sequencing (resulting sequence: SGNLESSLAP). A primary sequence database search indicated that the sequence belongs to a 69 residue hypothetical protein NE1300 in *N. europaea*. Proteolysis/MS of the gel band confirmed the candidate protein as full length NE1300 (Supporting Information Figure S7A). The electron density supported the modeling of 49 out of the 69 residues (residue 7−55) in the three equivalent copies of NE1300 (Figure 3).

DISCUSSION

The novel double cross-link model of heme P460 presented in this manuscript is also supported by the data that led to the previously proposed single cross-link model of HAO heme P460 (Figure 2 and 4B). A MS study demonstrated that cross-link formation led to the loss of two protons,[10] which for the double cross-link model is the C3 proton of the Tyr467′ ring and the Tyr467′ hydroxyl proton. In the new model, all four porphyrin *meso* carbons retain their proton upon cross-link formation, although the reported NMR data indicated that only three porphyrin *meso* protons were present in the aromatic region of the spectrum.[10] However, the NMR assignment was based on a reference system that assumed that C5 of the porphyrin remained part of an aromatic system. In the reference system, phenylhydrazine treated porphyrin-d_1 of cytochrome cd_1 generates a phenyl radical that regiospecifically replaces the porphyrin-C5 proton; thus, the porphyrin-C5 remains sp^2 hybridized.[31] As such, the additional complexity of porphyrin C4 and C5 becoming sp^3 hybridized was not anticipated. [It should be noted that with the loss of aromaticity, heme P460 is chemically no longer a heme (iron−porphyrin), but an iron−tetrapyrrole. We retain the heme nomenclature to reduce confusion with previous literature.] The Tyr hydroxyl proton undergoes solvent exchange, so no conclusion could be drawn about its presence/absence in the NMR study. In hindsight, the double cross-link model of heme P460 in HAO was also supported in the earlier 2.8 Å crystal structure, as the side chain oxygen of Tyr467′ is only 1.5 and 2.1 Å away from C4 of the porphyrin in the two NCS-related subunits.[5] Furthermore, the porphyrin-C5 geometry is more compatible with sp^3 rather than the sp^2 hybridization required to satisfy the original single cross-link model proposed (Figure 2).

Heme P460 of HAO exhibits a severe distortion of the macrocycle. Quantitative analysis using the normal-coordinate structural decomposition engine revealed that the main contribution to the deformation is *ruffling*, with an average distortion of 2.2 Å. Increased ruffling in *c*-type hemes correlates

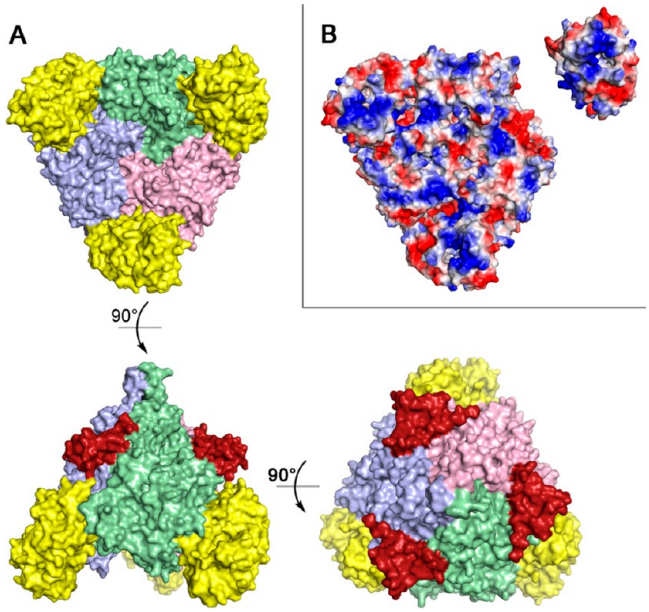

Figure 5. Surface rendering of the modeled HAO−NE1300−Cyt c_{554} complex. The HAO heme I porphyrin ring is ∼12 Å from the Cyt c_{554} heme I porphyrin ring. (A) The HAO trimer is colored by subunit (pink, green, and blue). The Cyt c_{554} is yellow, and the NE1300 is red. (B) The same view as the top figure in (A) that shows that vacuum electrostatics, but with one of the three Cyt c_{554} molecules separated from the complex. The figure was generated in PyMOL, http://www.pymol.org.[23]

dx.doi.org/10.1021/bi400960w | *Biochemistry* 2013, 52, 6211−6218

with lower midpoint redox potentials (E_m).[32] Heme P460 has an E_m of −260 mV versus the normal hydrogen electrode at pH 7, and is lower than typical *c*-type hemes, but is within the range of the other seven HAO *c*-type hemes (E_m ranging from +288 to −412 mV).[33] During turnover, it is postulated that a ferrous−NO heme P460 intermediate ($\{FeNO\}^7$ species) is oxidized to ferric−NO ($\{FeNO\}^6$ species), a step expected to be catalytically unfavorable. However, reaction of oxidized HAO with NO leads to a surprisingly stable $\{FeNO\}^6$ species.[34] Density functional theory (DFT) suggested that the ruffling of heme P460 destabilized the $\{FeNO\}^7$ intermediate and stabilized the $\{FeNO\}^6$ intermediate, enabling the oxidation step to occur at catalytic rates.[30] In addition, the ruffling appears to increase the affinity of heme P460 for its substrate, hydroxylamine. It should be noted that the chemically introduced electronic asymmetry may also be an important contributor to the ability of heme P460 to oxidize hydroxylamine.

How the tyrosine−porphyrin cross-links form is unknown. Heme P460 synthesis in Cyt P460 appears to be self-catalyzed, as the cross-link forms when the protein is overexpressed in *Pseudomonas aeruginosa*, an organism that contains neither HAO nor Cyt P460.[35] It is possible that the mechanism of heme P460 formation in HAO is also self-catalyzed through oxidation chemistry, most likely involving hydrogen peroxide. There is precedent in the literature for autocatalytic H_2O_2-dependent Tyr−heme cross-link formation.[36,37] In particular, the cross-link introduced into ascorbate peroxidase by site-directed mutagenesis demonstrated a tyrosyl radical mechanism, although it is unknown if this was generated via compound I (Fe(IV)=O with a porphyrin π−cation radical) or direct oxidation of the tyrosine by H_2O_2.[37] Interestingly, a consequence of ruffling is to favor the less common $(d_{xz},d_{yz})^4(d_{xy})^1$ configuration of low-spin ferric heme due to changes in orbital overlap.[38] This leads to a decrease in negative spin density on the heme *meso* carbons, which makes them more susceptible to oxidative attack.[32,38] This has functional precedence in the heme-degrading enzyme IsdI that induces a similar amount of ruffling (2.1 Å) as that observed in HAO heme P460, facilitating oxidation at the *meso* carbons.[39] Thus, the HAO protein environment may induce ruffling of the heme as a prerequisite to cross-link formation with Tyr467′. However, the double cross-link of HAO is more complex than the single Lys amine−porphyrin cross-link of Cyt P460, and so may require a processing enzyme. In the *hao* gene cluster, *orf2* always follows the *hao* gene.[40] It has no homology to known proteins, appears to be cytoplasmic membrane bound, and could potentially be a HAO maturation enzyme.

Because the HAO sample was purified from source (*N. europaea*), NE1300 is likely an interaction partner to HAO in vivo, though the biological function of NE1300 is unknown. The interaction between the proteins is strong because some NE1300 remains associated with HAO in SDS-PAGE gels as determined by MS (Supporting Information Figure S7B). It does not bind close to heme P460, and so is unlikely (at least directly) to be involved in its formation. NE1300 homologues (also classified as hypothetical proteins) do exist in two other bacteria of the *Nitrosomonas* genus (*N. eutropha* and *N. sp.*; 90 and 42% sequence identity, respectively). NE1300 and the homologous genes are all distant from the *hao* gene cluster, and the surrounding genes do not have any obvious connection to ammonia oxidation. Interestingly, the hypothesized docking site of Cyt c_{554} does not overlap with that of NE1300 (Figure 5).[7] In fact NE1300 lies adjacent to Cyt c_{554} in the HAO−NE1300−Cyt c_{554} complex model, and so might play a structural role in the electron transfer complex between Cyt c_{554} and HAO.

In summary, this study has demonstrated that the catalytic heme P460 of HAO possesses not only the single covalent cross-links to two Cys residues that define a *c*-type heme but also two additional cross-links to the side chain of a Tyr from the adjacent subunit. These additional cross-links undoubtedly lead to the unusual properties of HAO heme P460 and the ability to catalyze the oxidation of hydroxylamine to nitrite. Unexpectedly, each monomer of the trimeric HAO was bound to a small 69 residue protein identified as NE1300, a hypothetical protein of unknown function. As the HAO was purified from source, NE1300 is likely to be a biologically relevant partner.

■ ASSOCIATED CONTENT

Supporting Information

Previous crystal structure of HAO, mass spectrometry of HAO gel band, HAO transmembrane sequence prediction, photoreduction in HAO crystals, electron density of NE1300, SDS-PAGE showing presence of NE1300, and mass spectrometry of NE1300 gel band. This material is available free of charge via the Internet at http://pubs.acs.org.

Accession Codes

Coordinates and structure factors have been deposited in the Protein Data Bank as 4FAS.

■ AUTHOR INFORMATION

Corresponding Author

*C. M. Wilmot: e-mail, wilmo004@umn.edu; phone, (612) 624-2406.

Present Address

†Department of Structural Biology and Biophysics, Pfizer Global Research and Development, Groton, Connecticut 06340, United States.

Funding

This research was supported by the National Institute of General Medical Sciences of the National Institutes of Health under award numbers R01GM66569 and R01GM90260 (C.M.W.), an Office of the Dean of the Graduate School of the University of Minnesota Grant (A.B.H.) and Doctoral Dissertation Fellowship (P.C.), and a Minnesota Partnership for Biotechnology and Medical Genomics Grant SPAP-05−0013-P-FY06 (C.M.W.).

Notes

The authors declare no competing financial interest.

■ ACKNOWLEDGMENTS

We thank Stephan L. Ginell, Ph.D. and the staff at the SBC-CAT beamline 19-ID-D Argonne National Laboratory, Structural Biology Center at the Advanced Photon Source for valuable assistance during X-ray data collection. Argonne is operated by UChicago Argonne, LLC, for the U.S. Department of Energy, Office of Biological and Environmental Research under contract DE-AC02-06CH11357. Computer resources were provided by the Basic Sciences Computing Laboratory of the University of Minnesota Supercomputing Institute. We also thank Ed Hoeffner at the Kahlert Structural Biology Laboratory at the University of Minnesota.

■ ABBREVIATIONS:

HAO, hydroxylamine oxidoreductase; AMO, ammonia monooxygenase; Cyt c_{554}, cytochrome c_{554}; MS, mass spectrometry; NMR, nuclear magnetic resonance spectroscopy; Cyt P460, cytochrome P460; CCP4, Collaborative Computational Project Number 4; ASU, asymmetric unit; NCS, noncrystallographic symmetry; COOT, Crystallographic Object-Oriented Toolkit; NSD, normal-coordinate structure decomposition; E_m, midpoint redox potentials; DFT, density functional theory

■ REFERENCES

(1) Kowalchuk, G. A., and Stephen, J. R. (2001) Ammonia-oxidizing bacteria: a model for molecular microbial ecology. *Annu. Rev. Microbiol. 55*, 485−529.

(2) Andersson, K. K., Lipscomb, J. D., Valentine, M., Munck, E., and Hooper, A. B. (1986) Tetraheme cytochrome c-554 from *Nitrosomonas-europaea* - heme-heme interactions and ligand-binding. *J. Biol. Chem. 261*, 1126−1138.

(3) Yamanaka, T., and Shinra, M. (1974) Cytochrome c-552 and cytochrome c-554 derived from *Nitrosomonas europaea*. Purification, properties, and their function in hydroxylamine oxidation. *J. Biochem. 75*, 1265−1273.

(4) Hooper, A. B., Arciero, D. M., Bergmann, D. J., and Hendrich, M. P. (2005) *The oxidation of ammonia as an energy source in bacteria*, Vol. *16*, Springer, Dordrecht, Netherlands.

(5) Igarashi, N., Moriyama, H., Fujiwara, T., Fukumori, Y., and Tanaka, N. (1997) The 2.8 Å structure of hydroxylamine oxidoreductase from a nitrifying chemoautotrophic bacterium, *Nitrosomonas europaea*. *Nat. Struct. Biol. 4*, 276−284.

(6) Hooper, A. B., Tran, V. M., and Balny, C. (1984) Kinetics of reduction by substrate or dithionite and heme-heme electron transfer in the multiheme hydroxylamine oxidoreductase. *Eur. J. Biochem. 141*, 565−571.

(7) Iverson, T. M., Arciero, D. M., Hsu, B. T., Logan, M. S., Hooper, A. B., and Rees, D. C. (1998) Heme packing motifs revealed by the crystal structure of the tetra-heme cytochrome c554 from *Nitrosomonas europaea*. *Nat. Struct. Biol. 5*, 1005−1012.

(8) Rees, M., and Nason, A. (1965) A P-450-like cytochrome and a soluble terminal oxidase identified as cytochrome o from *Nitrosomonas europaea*. *Biochem. Biophys. Res. Commun. 21*, 248−256.

(9) Hooper, A. B., and Nason, A. (1965) Characterization of hydroxylamine-cytochrome c reductase from the chemoautotrophs *Nitrosomonas europaea* and *Nitrosocystis oceanus*. *J. Biol. Chem. 240*, 4044−4057.

(10) Arciero, D. M., Hooper, A. B., Cai, M., and Timkovich, R. (1993) Evidence for the structure of the active site heme P460 in hydroxylamine oxidoreductase of *Nitrosomonas*. *Biochemistry 32*, 9370−9378.

(11) Erickson, R. H., and Hooper, A. B. (1972) Preliminary characterization of a variant co-binding heme protein from *Nitrosomonas*. *Biochim. Biophys. Acta 275*, 231−244.

(12) Pearson, A. R., Elmore, B. O., Yang, C., Ferrara, J. D., Hooper, A. B., and Wilmot, C. M. (2007) The crystal structure of cytochrome P460 of *Nitrosomonas europaea* reveals a novel cytochrome fold and heme-protein cross-link. *Biochemistry 46*, 8340−8349.

(13) Numata, M., Saito, T., Yamazaki, T., Fukumori, Y., and Yamanaka, T. (1990) Cytochrome P-460 of *Nitrosomonas europaea*: further purification and further characterization. *J. Biochem. 108*, 1016−1021.

(14) Zahn, J. A., Duncan, C., and DiSpirito, A. A. (1994) Oxidation of hydroxylamine by cytochrome P-460 of the obligate methylotroph *Methylococcus capsulatus* Bath. *J. Bacteriol. 176*, 5879−5887.

(15) Arciero, D. M., and Hooper, A. B. (1997) Evidence for a crosslink between c-heme and a lysine residue in cytochrome P460 of *Nitrosomonas europaea*. *FEBS Lett. 410*, 457−460.

(16) Arciero, D. M., Balny, C., and Hooper, A. B. (1991) Spectroscopic and rapid kinetic studies of reduction of cytochrome c554 by hydroxylamine oxidoreductase from *Nitrosomonas europaea*. *Biochemistry 30*, 11466−11472.

(17) Cedervall, P. E., Hooper, A. B., and Wilmot, C. M. (2009) Crystallization and preliminary X-ray crystallographic analysis of a new crystal form of hydroxylamine oxidoreductase from *Nitrosomonas europaea*. *Acta Crystallogr., Sect. F: Struct. Biol. Cryst. Commun. F65*, 1296−1298.

(18) Otwinowski, Z., and Minor, W. (1997) Processing of X-ray Diffraction Data Collected in Oscillation Mode. *Methods Enzymol. 276*, 307−326.

(19) Winn, M. D., Ballard, C. C., Cowtan, K. D., Dodson, E. J., Emsley, P., Evans, P. R., Keegan, R. M., Krissinel, E. B., Leslie, A. G. W., McCoy, A., McNicholas, S. J., Murshudov, G. N., Pannu, N. S., Potterton, E. A., Powell, H. R., Read, R. J., Vagin, A., and Wilson, K. S. (2011) Overview of the CCP4 suite and current developments. *Acta Crystallogr., Sect. D: Biol. Crystallogr. D67*, 235−242.

(20) Emsley, P., and Cowtan, K. (2004) Coot: model-building tools for molecular graphics. *Acta Crystallogr., Sect. D: Biol. Crystallogr. D60*, 2126−2132.

(21) Murshudov, G. N., Vagin, A. A., and Dodson, E. J. (1997) Refinement of macromolecular structures by the maximum-likelihood method. *Acta Crystallogr., Sect. D: Biol. Crystallogr. D53*, 240−255.

(22) Winn, M. D., Isupov, M. N., and Murshudov, G. N. (2001) Use of TLS parameters to model anisotropic displacements in macromolecular refinement. *Acta Crystallogr., Sect. D: Biol. Crystallogr. D57*, 122−133.

(23) DeLano, W. L. (2002) *The PyMOL Molecular Graphics System*, Schrödinger, LLC, New York.

(24) Jentzen, W., Ma, J. G., and Shelnutt, J. A. (1998) Conservation of the conformation of the porphyrin macrocycle in hemoproteins. *Biophys. J. 74*, 753−763.

(25) Jentzen, W., Song, X. Z., and Shelnutt, J. A. (1997) Structural characterization of synthetic and protein-bound porphyrins in terms of the lowest-frequency normal coordinates of the macrocycle. *J. Phys. Chem. B 101*, 1684−1699.

(26) Tina, K. G., Bhadra, R., and Srinivasan, N. (2007) PIC: Protein Interactions Calculator. *Nucleic Acids Res. 35*, W473−476.

(27) Lyskov, S., and Gray, J. J. (2008) The RosettaDock server for local protein-protein docking. *Nucleic Acids Res. 36*, W233−238.

(28) McTavish, H., Arciero, D. M., and Hooper, A. B. (1995) Interaction with membranes of cytochrome c554 from *Nitrosomonas europaea*. *Arch. Biochem. Biophys. 324*, 53−58.

(29) Klotz, M. G., Schmid, M. C., Strous, M., op den Camp, H. J., Jetten, M. S., and Hooper, A. B. (2008) Evolution of an octahaem cytochrome c protein family that is key to aerobic and anaerobic ammonia oxidation by bacteria. *Environ. Microbiol. 10*, 3150−3163.

(30) Fernandez, M. L., Estrin, D. A., and Bari, S. E. (2008) Theoretical insight into the hydroxylamine oxidoreductase mechanism. *J. Inorg. Biochem. 102*, 1523−1530.

(31) Yap-Bondoc, F., and Timkovich, R. (1990) Inactivation of cytochrome cd1 by hydrazines. *J. Biol. Chem. 265*, 4247−4253.

(32) Liptak, M. D., Wen, X., and Bren, K. L. (2010) NMR and DFT investigation of heme ruffling: functional implications for cytochrome c. *J. Am. Chem. Soc. 132*, 9753−9763.

(33) Collins, M. J., Arciero, D. M., and Hooper, A. B. (1993) Optical spectropotentiometric resolution of the hemes of hydroxylamine oxidoreductase. Heme quantitation and pH dependence of E_m. *J. Biol. Chem. 268*, 14655−14662.

(34) Hendrich, M. P., Upadhyay, A. K., Riga, J., Arciero, D. M., and Hooper, A. B. (2002) Spectroscopic characterization of the NO adduct of hydroxylamine oxidoreductase. *Biochemistry 41*, 4603−4611.

(35) Bergmann, D. J., and Hooper, A. B. (2003) Cytochrome P460 of *Nitrosomonas europaea*. Formation of the heme-lysine cross-link in a heterologous host and mutagenic conversion to a non-cross-linked cytochrome c′. *Eur. J. Biochem. 270*, 1935−1941.

(36) Catalano, C. E., Choe, Y. S., and Demontellano, P. R. O. (1989) Reactions of the protein radical in peroxide-treated myoglobin - formation of a heme-protein cross-link. *J. Biol. Chem. 264*, 10534−10541.

(37) Pipirou, Z., Bottrill, A. R., Svistunenko, D. A., Efimov, I., Basran, J., Mistry, S. C., Cooper, C. E., and Raven, E. L. (2007) The reactivity of heme in biological systems: Autocatalytic formation of both tyrosine-heme and tryptophan-heme covalent links in a single protein architecture. *Biochemistry 46*, 13269−13278.
(38) Nakamura, M. (2006) Electronic structures of highly deformed iron(III) porphyrin complexes. *Coord. Chem. Rev. 250*, 2271−2294.
(39) Takayama, S. J., Ukpabi, G., Murphy, M. E. P., and Mauk, A. G. (2011) Electronic properties of the highly ruffled heme bound to the heme degrading enzyme IsdI. *Proc. Natl. Acad. Sci. U. S. A. 108*, 13071−13076.
(40) Bergmann, D. J., Hooper, A. B., and Klotz, M. G. (2005) Structure and sequence conservation of *hao* cluster genes of autotrophic ammonia-oxidizing bacteria: evidence for their evolutionary history. *Appl. Environ. Microbiol. 71*, 5371−5382.